Non-Abelian A_4 vortices in $SO(3)$ gauge theory and noninvertible symmetries

Yoshihiko Abe,[1,2,3,*] Tetsutaro Higaki,[4,5,†] Kazuya Murakami,[4,‡] Muneto Nitta,[6,5,7,§] and Ryo Yokokura[6,5,‖]

[1]*Graduate School of Science and Technology, Keio University, Yokohama, Kanagawa 223-8522, Japan*
[2]*Keio University Sustainable Quantum Artificial Intelligence Center (KSQAIC), Keio University, Tokyo 108-8345, Japan*
[3]*Quantum Computing Center, Keio University, 3-14-1 Hiyoshi, Kohoku-ku, Yokohama, Kanagawa 223-8522, Japan*
[4]*Department of Physics, Keio University, Yokohama 223-8533, Japan*
[5]*Research and Education Center for Natural Sciences, Keio University, 4-1-1 Hiyoshi, Yokohama, Kanagawa 223-8521, Japan*
[6]*Department of Physics, Keio University, 4-1-1 Hiyoshi, Yokohama, Kanagawa 223-8521, Japan*
[7]*International Institute for Sustainability with Knotted Chiral Meta Matter (WPI-SKCM^2), Hiroshima University, 1-3-1 Kagamiyama, Higashi-Hiroshima, Hiroshima 739-8531, Japan*

(Received 21 July 2026; accepted 1 October 2026; published 4 November 2026)

We construct finite-tension non-Abelian vortex solutions in a renormalizable $(3+1)$-dimensional $SO(3)$ gauge theory Higgsed to the tetrahedral group A_4 by a Higgs field in the spin-3 representation. Since the vacuum manifold is $SO(3)/A_4$, the vortices are characterized by the non-Abelian fundamental group $\pi_1(SO(3)/A_4) \simeq \tilde{A}_4$, the binary tetrahedral group. We obtain explicit axisymmetric vortex solutions carrying holonomies corresponding to the order-two and order-three conjugacy classes of A_4, determine their tensions numerically, and show that they exhibit type-I, type-II, and Bogomol'nyi-Prasad-Sommerfield-like behavior depending on the Higgs and gauge boson mass ratios. The vortices are classified by conjugacy classes of $\tilde{A}_4$, while their infrared descriptions are labeled by conjugacy classes of A_4. We further demonstrate that the smooth finite-tension vortices reduce in the infrared to Gukov-Witten surface operators of the A_4 discrete gauge theory, thereby establishing a finite-energy ultraviolet completion of noninvertible defects in a renormalizable gauge-Higgs theory.

DOI: 10.1103/bz2v-mls7

I. INTRODUCTION AND SUMMARY

Topological solitons, which are classical solutions with topological charges, have been extensively studied in past decades [1–3]. Among others, vortices can often arise in many contexts such as superconductors, superfluids, cosmic strings, and so on [4,5]. Here, they are codimension-2 objects whose topological charges are winding numbers. It has been known that a non-Abelian fundamental group $\pi_1(G/H)$ of a non-Abelian symmetry group G and its unbroken subgroup H allows non-Abelian vortices exhibiting exotic properties such as non-Abelian fusion and braiding rules [6–15].[1] Global analogs of such non-Abelian vortices were first found in condensed matter physics [28]: liquid crystals [28–32], and Bose-Einstein condensates (BECs) [33–40], as well as in nuclear and astrophysics such as $^3P_2$ neutron superfluids in neutron stars [41–47]. In $(3+1)$ dimensions, the collision of two vortices corresponding to noncommutative π_1 elements results in a rung vortex [28,29,34], and consequently, in cosmology, it yields a non-Abelian cosmic string network [15]. In addition, non-Abelian vortex knots are also possible [13,38–40].

In gauge theories with gauge group G Higgsed to H, non-Abelian vortices exhibit non-Abelian Aharonov-Bohm (AB) effects if $\pi_1(G/H)$ is non-Abelian [48–53]. The low-energy limit of the Higgs phase can be described by an H gauge theory where there are no local fluctuations if H

*Contact author: yabe3@keio.jp
†Contact author: thigaki@rk.phys.keio.ac.jp
‡Contact author: kazuyamurakami@keio.jp
§Contact author: mune.nitta@gmail.com
‖Contact author: ryokokur@keio.jp

Published by the American Physical Society under the terms of the Creative Commons Attribution 4.0 International license. Further distribution of this work must maintain attribution to the author(s) and the published article's title, journal citation, and DOI. Funded by SCOAP^3.

[1]Note that the terminology "non-Abelian vortices" implies another meaning in other contexts such as supersymmetric QCD [16–21] and dense QCD [22–27], where even though $\pi_1(G/H)$ is Abelian, vortices are called non-Abelian in the sense that H is non-Abelian and they carry non-Abelian moduli.

is a discrete group [54]. The non-Abelian fusion and braiding rules of the vortices in the gauge theories have been discussed in terms of the AB effects for charged particles far from the vortices. However, to the best of our knowledge, explicit vortex solutions with non-Abelian $\pi_1(G/H)$ have not been constructed so far. Thus, several important physical properties, such as their tensions and the interactions between vortices, have remained unclear.

In this article, we derive the vortex solutions with non-Abelian $\pi_1(G/H)$ in a Higgs phase of a $(3+1)$-dimensional gauge theory. We focus on an $SO(3)$ gauge theory Higgsed to the tetrahedral group A_4, where $\pi_1(SO(3)/A_4)$ is non-Abelian. The discrete group A_4 has been widely used in particle-physics flavor models and, more recently, in models based on modular symmetry [55–57]. $SO(3)$ gauge theories Higgsed to A_4 have also been studied in particle physics [58–60].[2] We show that the vortex solutions can be classified by the conjugacy class of the un-Higgsed subgroup A_4, and the non-Abelian AB effects can be expressed by the indicator of A_4. This is the first explicit finite-tension realization of non-Abelian vortices whose non-Abelianity originates solely from a non-Abelian fundamental group.

Using the field configurations of the vortices, we discuss the tensions of the vortices. The tensions depend on the ratio of the masses of the Higgs field and the gauge field. The dependence implies that the vortices are attractive for a large gauge field mass and repulsive for a large Higgs field mass. We find that there are no attractive or repulsive forces if the mass of the gauge field is equal to that of the Higgs field. In this case, the vortices might be understood as Bogomol'nyi-Prasad-Sommerfield (BPS) states. See, e.g., Refs. [20,21] as a review for BPS vortices. However, our vortices are quite different from conventional BPS states because the mass-charge relations do not hold due to $\pi_1(G/H) \not\cong \mathbb{Z}$.

Finally, we discuss our vortex solutions from the viewpoint of generalized global symmetries [61]. It has been known that the A_4 gauge theory possesses a noninvertible one-form symmetry, whose symmetry generators are the so-called Gukov-Witten operators, which produce non-Abelian AB effects for test particles [62,63]. We find that the non-Abelian vortices exhibit the same fusion rule and the non-Abelian AB effects as the Gukov-Witten operators. This coincidence means that the Gukov-Witten operators can be realized as the low-energy limit of the non-Abelian vortices. Since our gauge-Higgs system is a renormalizable UV completion of the infrared A_4 gauge theory, the noninvertible one-form symmetry, which emerges only in the Higgs phase, does not survive once the gauge group $SO(3)$ is un-Higgsed, for example, at sufficiently high energies. In the infrared A_4 gauge theory, the noninvertible one-form symmetry is explicitly broken in the presence of dynamical matter fields.

This article is organized as follows. In Sec. II, we introduce our model. Using the model, the vortex solutions are established in Sec. III. We then calculate the tensions of the vortices, and find type-I, -II, and BPS-like vortices in Sec. IV. The topological classification of the vortices is discussed in Sec. V. In Sec. VI, we relate our vortex solutions to the noninvertible symmetries. Finally, we discuss our results in Sec. VII. In Appendix A, we give the explicit 7×7 matrices representing the Lie algebra in the spin-3 representation. In Appendix B, we write down our Higgs potential explicitly. The uniqueness of the profile for a Higgs field needed in Sec. III is derived in Appendix C.

II. MODEL

We consider the following $SO(3)$ gauge-Higgs system in $3+1$ dimensions, with Lagrangian density

$$\mathcal{L} = -\frac{1}{4e^2} G^a_{\mu\nu} G^{a\mu\nu} - \frac{1}{2} D_\mu \phi_A D^\mu \phi_A - V(\phi). \tag{1}$$

Here e is the gauge coupling, and ϕ is a Higgs field in the spin-3 irreducible representation of $SO(3)$. We expand it as

$$\phi(x) = \sum_{A=1}^{7} \phi_A(x) e_A, \tag{2}$$

where e_A, $A = 1, \ldots, 7$, is an orthonormal basis of the spin-3 representation space introduced below.

We write the $SO(3)$ gauge field as

$$W_\mu = W^a_\mu T^a. \tag{3}$$

We take iT^a to be the following generators of the Lie algebra $\mathfrak{so}(3)$:

$$iT^1 = \begin{pmatrix} 0 & 0 & 0 \\ 0 & 0 & 1 \\ 0 & -1 & 0 \end{pmatrix}, \qquad iT^2 = \begin{pmatrix} 0 & 0 & -1 \\ 0 & 0 & 0 \\ 1 & 0 & 0 \end{pmatrix},$$
$$iT^3 = \begin{pmatrix} 0 & 1 & 0 \\ -1 & 0 & 0 \\ 0 & 0 & 0 \end{pmatrix}. \tag{4}$$

With this convention, the field-strength components are

$$G^a_{\mu\nu} = \partial_\mu W^a_\nu - \partial_\nu W^a_\mu - \varepsilon^{abc} W^b_\mu W^c_\nu, \tag{5}$$

where ε^{abc} is the totally antisymmetric tensor with $\varepsilon^{123} = 1$.

A gauge transformation is given by an $SO(3)$-valued function $U(x)$. With our convention, it acts on the fields as

[2] In condensed matter physics, similar A_4 vortices exist in the so-called cyclic phase of spin-2 BECs in which $U(1)\times SO(3)$ is broken to a subgroup containing A_4 (often denoted by T in that context) [33–35,37,40].

$$W_\mu \longmapsto U W_\mu U^{-1} + i(\partial_\mu U)U^{-1}, \tag{6}$$

$$\phi \longmapsto \rho(U)\phi, \tag{7}$$

where ρ denotes the spin-3 representation of $SO(3)$.

We now describe the spin-3 representation more explicitly. We denote its representation space by $\mathcal{H}_3$. It can be realized as the space of real harmonic homogeneous polynomials of degree three in three variables,

$$\mathcal{H}_3 := \{f \in \mathbb{R}[\mathcal{X}, \mathcal{Y}, \mathcal{Z}] | \deg f = 3, \Delta f = 0\}. \tag{8}$$

The $SO(3)$ action is given by

$$(\rho(g)f)((\mathcal{X}, \mathcal{Y}, \mathcal{Z})^T) = f(g^{-1}(\mathcal{X}, \mathcal{Y}, \mathcal{Z})^T), \qquad g \in SO(3). \tag{9}$$

With this action, the covariant derivative is

$$D_\mu \phi_A = \partial_\mu \phi_A + W^a_\mu (X_a)_{AB} \phi_B, \tag{10}$$

where X_a are the 7×7 matrices representing the Lie algebra in the spin-3 representation. Their explicit form is given in Appendix A.

We define the $SO(3)$-invariant inner product by

$$\langle f, g \rangle := \frac{1}{4\pi} \int_{S^2} f(\mathcal{X}, \mathcal{Y}, \mathcal{Z}) g(\mathcal{X}, \mathcal{Y}, \mathcal{Z}) d\Omega, \tag{11}$$

where $S^2 \subset \mathbb{R}^3$ is the unit sphere,

$$S^2 = \{(\mathcal{X}, \mathcal{Y}, \mathcal{Z}) \in \mathbb{R}^3 | \mathcal{X}^2 + \mathcal{Y}^2 + \mathcal{Z}^2 = 1\}, \tag{12}$$

and $d\Omega$ denotes its standard area element. With respect to this inner product, we use the following orthonormal basis of $\mathcal{H}_3$:

$$\begin{aligned}
e_1 &= \sqrt{7}\left(\mathcal{X}^3 - \frac{3}{2}\mathcal{X}(\mathcal{Y}^2 + \mathcal{Z}^2)\right) \\
e_2 &= \sqrt{7}\left(\mathcal{Y}^3 - \frac{3}{2}\mathcal{Y}(\mathcal{Z}^2 + \mathcal{X}^2)\right) \\
e_3 &= \sqrt{7}\left(\mathcal{Z}^3 - \frac{3}{2}\mathcal{Z}(\mathcal{X}^2 + \mathcal{Y}^2)\right) \\
e_4 &= \frac{\sqrt{105}}{2}\mathcal{X}(\mathcal{Y}^2 - \mathcal{Z}^2) \\
e_5 &= \frac{\sqrt{105}}{2}\mathcal{Y}(\mathcal{Z}^2 - \mathcal{X}^2) \\
e_6 &= \frac{\sqrt{105}}{2}\mathcal{Z}(\mathcal{X}^2 - \mathcal{Y}^2) \\
e_7 &= \sqrt{105}\mathcal{X}\mathcal{Y}\mathcal{Z}.
\end{aligned} \tag{13}$$

For $\phi \in \mathcal{H}_3$, we define

$$I_n(\phi) := \frac{1}{4\pi} \int_{S^2} \phi(\mathcal{X}, \mathcal{Y}, \mathcal{Z})^n d\Omega. \tag{14}$$

In particular, if $\phi = \sum_{A=1}^7 \phi_A e_A$, then

$$I_2(\phi) = \langle \phi, \phi \rangle = \sum_{A=1}^7 \phi_A^2. \tag{15}$$

The $SO(3)$-invariant polynomials on $\mathcal{H}_3$ of degree at most four are spanned by

$$1, \qquad I_2, \qquad I_2^2, \qquad I_4. \tag{16}$$

For the spin-3 representation, representation theory gives

$$\min_{\phi \in \mathcal{H}_3 \setminus \{0\}} \frac{I_4(\phi)}{I_2(\phi)^2} = \frac{315}{143}. \tag{17}$$

We therefore normalize the quartic invariant as

$$Q(\phi) := \frac{143}{315} I_4(\phi) - I_2(\phi)^2. \tag{18}$$

With this normalization,

$$Q(\phi) \geq 0. \tag{19}$$

An explicit component expression for Q is given in Appendix B. Using these invariants, we take the Higgs potential to be

$$\begin{aligned}
V(\phi) &= \gamma Q(\phi) - \mu^2 I_2(\phi) + \lambda I_2(\phi)^2 + \frac{\mu^4}{4\lambda} \\
&= \gamma Q(\phi) + \lambda(I_2(\phi) - v^2)^2,
\end{aligned} \tag{20}$$

where

$$\gamma > 0, \qquad \lambda > 0, \qquad \mu^2 > 0, \qquad v^2 = \frac{\mu^2}{2\lambda}. \tag{21}$$

With this choice, the vacuum expectation value of the Higgs field is

$$\langle \phi \rangle = v e_7, \tag{22}$$

up to an $SO(3)$ gauge transformation. Since $e_7 \propto \mathcal{X}\mathcal{Y}\mathcal{Z}$, only a finite subgroup of $SO(3)$ leaves this vacuum invariant. The remaining gauge symmetry is the tetrahedral group A_4, generated for example by

$$r_2 = \begin{pmatrix} -1 & 0 & 0 \\ 0 & -1 & 0 \\ 0 & 0 & 1 \end{pmatrix}, \qquad r_3 = \begin{pmatrix} 0 & 0 & 1 \\ 1 & 0 & 0 \\ 0 & 1 & 0 \end{pmatrix}. \tag{23}$$

The first generator is a π-rotation around the (0, 0, 1)-axis, and the second is a $2\pi/3$-rotation around the (1, 1, 1)-axis. These generators satisfy

$$r_2^2 = r_3^3 = (r_2 r_3)^3 = 1_{3\times 3}, \tag{24}$$

which are the defining relations of A_4. Thus, the Higgs mechanism breaks the gauge symmetry as

$$SO(3) \to A_4. \tag{25}$$

The corresponding vacuum manifold is

$$\mathcal{M} \simeq SO(3)/A_4. \tag{26}$$

The topological classification of finite-tension string configurations will be discussed in Sec. V. In the next section, we construct explicit axisymmetric vortex solutions with asymptotic holonomies r_2^n and r_3^m in A_4.

III. VORTEX SOLUTIONS

We now construct static, z-independent, axisymmetric vortex solutions in the Higgs phase. Let (r, θ, z) be cylindrical coordinates with the vortex aligned along the z-axis, where the vortex core is located at $r = 0$. The finite-tension condition requires that, as $r \to \infty$, the Higgs field approaches the vacuum manifold. Thus, when one goes around a large circle C_∞ linking the vortex, the Higgs field may return to itself up to an element of the un-Higgsed group A_4. Equivalently, the asymptotic gauge holonomy

$$U_\infty = \mathrm{P}\exp\left(-i\oint_{C_\infty} W_\mu\, dx^\mu\right) \tag{27}$$

must belong to A_4. Physically, a nontrivial U_∞ represents magnetic flux carried along the vortex line.

Before presenting the vortex *Ansätze*, we introduce the mass parameters and dimensionless variables used in the radial equations. Expanding the Higgs potential around the vacuum $\phi = v e_7$, the Hessian with respect to the orthonormal basis $e_1, \ldots, e_7$ is

$$\mathrm{Hess}V|_{ve_7} = \mathrm{diag}(m_-^2, m_-^2, m_-^2, 0, 0, 0, m_+^2). \tag{28}$$

The three zero modes e_4, e_5, e_6 are the would-be Nambu-Goldstone directions associated with the broken $SO(3)$ generators and are eaten by the gauge field. The two Higgs-sector mass scales are

$$m_+ = 2\mu, \qquad m_- = \frac{4}{3\sqrt{5}}\frac{\mu\sqrt{\gamma}}{\sqrt{\lambda}}. \tag{29}$$

The Higgs mechanism also gives a common mass to the three gauge bosons,

$$m_G = \frac{\sqrt{2}\mu e}{\sqrt{\lambda}}. \tag{30}$$

We define the dimensionless radial coordinate by

$$R = e v\, r = \frac{m_G r}{2}, \tag{31}$$

and introduce the dimensionless mass ratios

$$\kappa := \frac{m_+}{m_G}, \qquad \eta := \frac{m_+}{m_-}. \tag{32}$$

A. Order-two vortex family

We begin with a vortex family whose asymptotic holonomy is given by the Nth power of a fixed order-two element of A_4. For a positive integer N, we take

$$W_\mu dx^\mu = -\frac{N}{2}K(r)T^3 d\theta, \tag{33}$$

$$\phi = v h(r)(\sin N\theta e_6 + \cos N\theta e_7). \tag{34}$$

The finite-tension condition and continuity at the vortex core lead to the boundary conditions:

$$K(0) = 0, \qquad K(\infty) = 1, \tag{35}$$

$$h(0) = 0, \qquad h(\infty) = 1. \tag{36}$$

The holonomy around a large circle is

$$U_\infty = \exp(N\pi i T^3) = \begin{pmatrix} -1 & 0 & 0 \\ 0 & -1 & 0 \\ 0 & 0 & 1 \end{pmatrix}^N. \tag{37}$$

Thus, the $SO(3)$ holonomy is the N-th power of an order-two element of A_4. We refer to this family as the order-two family. The radial equations are obtained by substituting the *Ansatz* into the Euler-Lagrange equations:

$$0 = -K'' + \frac{K'}{R} + 4h^2(K-1), \tag{38}$$

$$0 = h'' + \frac{h'}{R} - \frac{N^2(K-1)^2 h}{R^2} + 2\kappa^2(1-h^2)h. \tag{39}$$

Here and below, a prime denotes differentiation with respect to R.

We now examine the asymptotic behavior of the profile functions. First, linearizing the equations around the vacuum at spatial infinity, we find

$$K(R) = 1 - C_G e^{-2R} + \cdots, \tag{40}$$

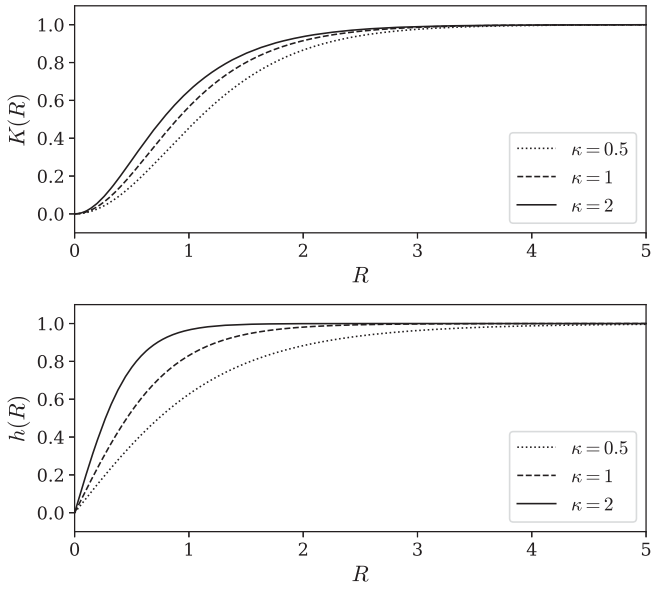


FIG. 1. Numerical profiles $K(R)$ and $h(R)$ of the order-two vortex with $N = 1$ for $\kappa = 0.5$, 1, 2.

$$h(R) = 1 - C_+ e^{-2\kappa R} + \cdots. \tag{41}$$

Near the origin, expanding the reduced equations around $R = 0$, one finds

$$K(R) = K_2 R^2 + O(R^4), \quad h(R) = h_N R^N + O(R^{N+2}). \tag{42}$$

Here, C_G, C_+, K_2, and h_N are constants. This shows that the configuration is smooth in Cartesian coordinates near the core.

Solving the above boundary value problem numerically, we obtain the representative profile shown in Fig. 1. In the numerical calculation, the boundary conditions at infinity are imposed at a finite cutoff $R_{\max}$, chosen sufficiently large for the profiles to reach their asymptotic values.

B. Order-three vortex family

We next turn to a vortex family whose asymptotic holonomy is given by the Mth power of a fixed order-three element of A_4. Let

$$T^\Delta := T^1 + T^2 + T^3. \tag{43}$$

For a positive integer M, we take

$$W_\mu dx^\mu = -\frac{M\sqrt{3}}{9} K(r) T^\Delta d\theta, \tag{44}$$

$$\phi = v \begin{pmatrix} \frac{2\sqrt{15}}{27}(a(r)\cos M\theta - b(r)) \\ \frac{2\sqrt{15}}{27}(a(r)\cos M\theta - b(r)) \\ \frac{2\sqrt{15}}{27}(a(r)\cos M\theta - b(r)) \\ \frac{2\sqrt{3}}{9} a(r)\sin M\theta \\ \frac{2\sqrt{3}}{9} a(r)\sin M\theta \\ \frac{2\sqrt{3}}{9} a(r)\sin M\theta \\ \frac{4}{9} a(r)\cos M\theta + \frac{5}{9} b(r) \end{pmatrix}. \tag{45}$$

The finite-tension condition and continuity at the vortex core lead to the boundary conditions:

$$K(0) = 0, \qquad K(\infty) = 1, \tag{46}$$

$$a(0) = 0, \qquad a(\infty) = 1, \tag{47}$$

$$b'(0) = 0, \qquad b(\infty) = 1. \tag{48}$$

The holonomy around a large circle is

$$U_\infty = \exp\left(\frac{2M\pi\sqrt{3}}{9} i(T^1 + T^2 + T^3)\right) = \begin{pmatrix} 0 & 0 & 1 \\ 1 & 0 & 0 \\ 0 & 1 & 0 \end{pmatrix}^M. \tag{49}$$

Thus the $SO(3)$ holonomy is the Mth power of an order-three element of A_4. We refer to this family as the order-three family.

Substituting this *Ansatz* into the full Euler-Lagrange equations, one finds

$$0 = K'' - \frac{K'}{R} - 4a^2(K-1), \tag{50}$$

$$0 = -a'' - \frac{a'}{R} + \frac{M^2(K-1)^2 a}{R^2} + \frac{2\kappa^2(-9 + 4a^2 + 5b^2)a}{9} + \frac{10\kappa^2(a^2 - b^2)a}{9\eta^2}, \tag{51}$$

$$0 = -b'' - \frac{b'}{R} + \frac{2\kappa^2(-9 + 4a^2 + 5b^2)b}{9} - \frac{8\kappa^2(a^2 - b^2)b}{9\eta^2}. \tag{52}$$

We now examine the asymptotic behavior of the profile functions. At spatial infinity, it is useful to introduce

$$h_+ := \frac{4a + 5b}{9}, \qquad h_- := a - b. \tag{53}$$

Linearizing the equations around the vacuum $K = a = b = 1$, we find

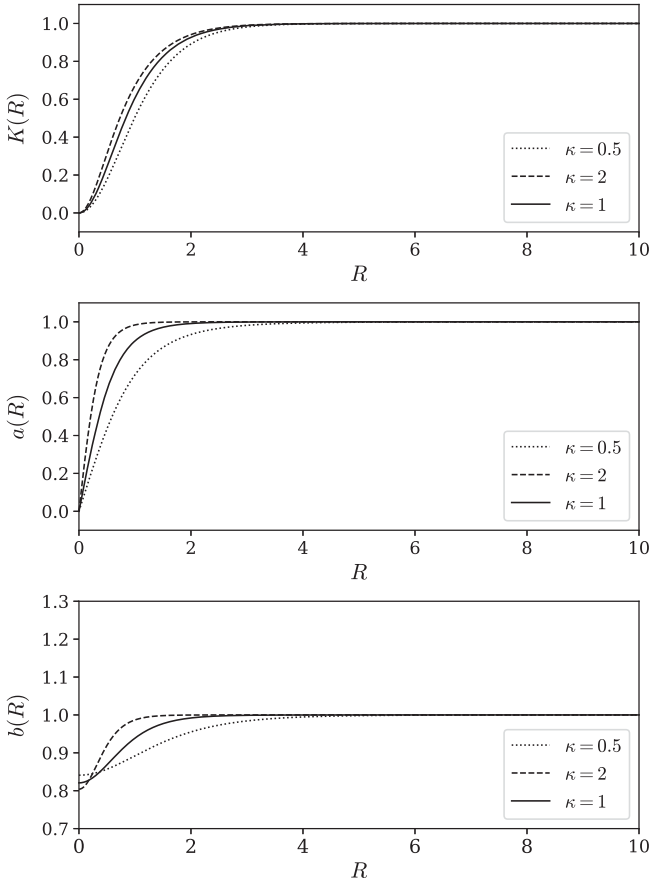


FIG. 2. Representative numerical profiles for the order-three vortex *Ansatz* with $M = 1$ and $\eta = 0.5$. The profiles are shown for $\kappa = 0.5$, 1, 2.

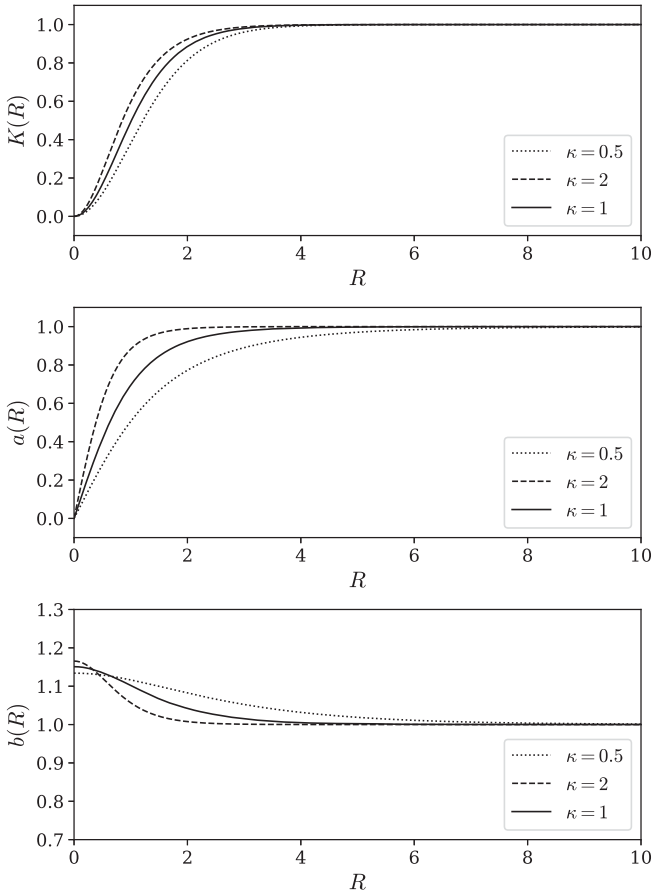


FIG. 3. Representative numerical profiles for the order-three vortex *Ansatz* with $M = 1$ and $\eta = 2$. The profiles are shown for $\kappa = 0.5$, 1, 2.

$$K(R) = 1 - C_G e^{-2R} + \cdots, \tag{54}$$

$$h_+(R) = 1 - C_+ e^{-2\kappa R} + \cdots, \tag{55}$$

$$h_-(R) = C_- e^{-2\kappa R/\eta} + \cdots. \tag{56}$$

Near the origin, expanding the reduced equations around $R = 0$, one finds

$$K(R) = K_2 R^2 + O(R^4), \tag{57}$$

$$a(R) = a_M R^M + O(R^{M+2}), \tag{58}$$

$$b(R) = b_0 + O(R^2). \tag{59}$$

Here, C_G, $C_\pm$, K_2, a_M and b_0 are constants. This near-core behavior shows that the configuration is smooth in Cartesian coordinates.

There is a useful special case at $\eta = 1$. In this case the b-equation decouples from K and a. Moreover, the only regular finite-tension solution satisfying the boundary conditions is

$$b(R) \equiv 1. \tag{60}$$

We prove this uniqueness statement in Appendix C. The remaining equations for K and a then take exactly the same form as those of the order-two family, after the identification

$$M \leftrightarrow N, \qquad a \leftrightarrow h. \tag{61}$$

Representative numerical profiles obtained by solving the boundary value problem are shown in Figs. 2 and 3.

IV. TYPE-I, -II, AND BPS-LIKE VORTICES

We now discuss the energetics of the order-two and order-three vortex families constructed above. Both families exhibit type-I/type-II-like energetics, with BPS-like points appearing at special values of the mass ratios. Here we use the terms type-I, type-II, and BPS-like in analogy with the Abelian-Higgs model [4,5], or equivalently with the Ginzburg-Landau theory of superconductivity. More precisely, type-I-like behavior means that vortices at infinite separation have higher total tension than the corresponding

combined vortex, whereas type-II-like behavior means that the infinitely separated configuration has lower tension. By a BPS-like point, we mean a point at which the reduced energy has a Bogomol'nyi-type structure and the binding energy between vortices vanishes. As will be shown below, the BPS-like points occur at $\kappa = 1$ for the order-two family and at $(\eta, \kappa) = (1, 1)$ for the order-three family.

The energy functional associated with the Lagrangian (1) is

$$E = \int d^3x \left[\frac{1}{2e^2} ((\mathcal{E}_i^a)^2 + (\mathcal{B}_i^a)^2) + \frac{1}{2} ((D_0\phi_A)^2 + (D_i\phi_A)^2) + V(\phi) \right], \tag{62}$$

where

$$\mathcal{E}_i^a := G_{0i}^a, \qquad \mathcal{B}_i^a := -\frac{1}{2}\varepsilon_{ijk} G_{jk}^a. \tag{63}$$

For the order-two family, substituting *Ansatz* (33) and (34) into (62), one obtains

$$E = \frac{\pi\mu^2}{2\lambda} \int dz\, E_2(N;\kappa), \tag{64}$$

where $E_2(N;\kappa)$ is the dimensionless tension,

$$E_2(N;\kappa) := \int_0^\infty \left[\frac{N^2(K')^2}{4R^2} + (h')^2 + \frac{N^2(K-1)^2h^2}{R^2} + \kappa^2(h^2-1)^2 \right] R\, dR. \tag{65}$$

This functional has the same form as the energy functional of the Abelian-Higgs vortex. The mass ratio $\kappa = \frac{m_+}{m_G}$ in Eq. (32) plays the role of the Ginzburg-Landau parameter. The integer N plays the same role as the usual Abelian-Higgs winding number. However, in the full $SO(3) \to A_4$ theory, N is not itself a $\mathbb{Z}$-valued topological charge. The actual topological sector is discussed in Sec. V.

We determine the type-I/type-II-like behavior by comparing the tension $E_2(N;\kappa)$ of the configuration labeled by N with $NE_2(1;\kappa)$, the tension of N copies of the $N = 1$ configuration at infinite separation. This comparison is shown in Fig. 4. When

$$E_2(N;\kappa) < N\, E_2(1;\kappa), \tag{66}$$

the combined configuration has lower tension, corresponding to type-I-like behavior. Conversely, when

$$E_2(N;\kappa) > N\, E_2(1;\kappa), \tag{67}$$

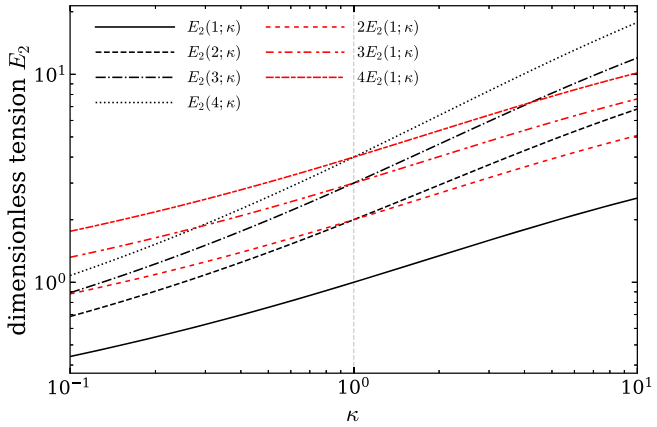


FIG. 4. Tension comparison for the order-two family as a function of κ. We compare $E_2(N;\kappa)$, the tension of the configuration labeled by N, with $NE_2(1;\kappa)$, the total tension of N copies of the $N = 1$ configuration at infinite separation.

the infinitely separated configuration is energetically favored, corresponding to type-II-like behavior. As seen in Fig. 4, the transition between the type-I-like and type-II-like regimes occurs at $\kappa = 1$. At this point, the reduced energy (65) admits the standard Abelian-Higgs Bogomol'nyi completion, giving

$$E_2(N;1) = N. \tag{68}$$

Thus, the binding energy between vortices vanishes at $\kappa = 1$, exactly as at the Bogomol'nyi point of the Abelian-Higgs model.

For the order-three family, substituting *Ansatz* (44) and (45) into (62), one obtains

$$E = \frac{\pi\mu^2}{2\lambda} \int dz\, E_3(M;\eta,\kappa), \tag{69}$$

where $E_3(M;\eta,\kappa)$ is the dimensionless tension,

$$E_3(M;\eta,\kappa) := \frac{4}{9}\int_0^\infty \left[\frac{M^2(K')^2}{4R^2} + (a')^2 + \frac{5}{4}(b')^2 + \frac{M^2(K-1)^2a^2}{R^2} + \frac{\kappa^2(-9+4a^2+5b^2)^2}{36} + \frac{5\kappa^2(a^2-b^2)^2}{9\eta^2} \right] R\, dR. \tag{70}$$

Unlike the order-two family, this functional contains two scalar profiles, $a(R)$ and $b(R)$. Therefore, for generic η, it is not equivalent to a single-component Abelian-Higgs vortex. There is, however, a special simplification at $\eta = 1$. In this case, regularity at the vortex core and finite tension imply

$$b(R) \equiv 1, \tag{71}$$

as shown in the previous section. The dimensionless tension (70) then reduces to

$$E_3(M;1,\kappa)=\frac{4}{9}\int_0^\infty\left[\frac{M^2(K')^2}{4R^2}+(a')^2+\frac{M^2(K-1)^2a^2}{R^2}+\kappa^2(a^2-1)^2\right]R\,dR. \quad (72)$$

This is identical to (65), up to the overall factor $4/9$, under the identification

$$M\leftrightarrow N, \qquad a\leftrightarrow h. \quad (73)$$

Hence

$$E_3(M;1,\kappa)=\frac{4}{9}E_2(M;\kappa). \quad (74)$$

Combining this relation with (68), we obtain, at $\kappa=1$,

$$E_3(M;1,1)=\frac{4}{9}M. \quad (75)$$

Thus, within the order-three family, the point $(\eta,\kappa)=(1,1)$ is BPS-like: the reduced energy functional has an Abelian-Higgs Bogomol'nyi structure, the tension is linear in the vortex label M, and the binding energy between separated vortices vanishes.

The analytic results at the BPS-like points provide useful benchmarks for testing the numerical accuracy. We verify that the numerical tensions agree with the analytic results (68) and (75) with relative errors below 10^{-5}. A representative convergence test is presented in Appendix D.

V. TOPOLOGICAL CLASSIFICATION

We now classify the vortex solutions constructed above. A string configuration defines, at spatial infinity, a loop in the vacuum manifold $\mathcal{M}=SO(3)/A_4$. Let $p:SU(2)\to SO(3)$ denote the double covering map. Since $SU(2)$ is simply connected, we have

$$\pi_1(\mathcal{M})=\pi_1(SO(3)/A_4)\simeq p^{-1}(A_4)=:\tilde{A}_4, \quad (76)$$

where $\tilde{A}_4$ is the binary tetrahedral group, $\tilde{A}_4\simeq SL(2,3)$. (See, for instance, Refs. [37,43,57].) Thus the loop at spatial infinity determines an element of $\tilde{A}_4$. However, a gauge transformation at spatial infinity conjugates this element. Therefore physical string configurations are labeled by conjugacy classes of $\tilde{A}_4$, rather than by individual elements.

Since the gauge group is $SO(3)$, genuine Wilson lines are labeled only by integer-spin representations. Therefore they can detect only the conjugacy class of the projected $SO(3)$ holonomy in A_4, not the full topological class in $\tilde{A}_4$. In particular, the two classes in $\tilde{A}_4$ that project to the same class in A_4 cannot be distinguished by such Wilson loops, although they may represent different topological sectors of the Higgs configuration.

We now make explicit the relation between the projected $SO(3)$ holonomy and the topological class in $\tilde{A}_4=p^{-1}(A_4)\simeq\pi_1(SO(3)/A_4)$.

Throughout this section, $[g]$ denotes the conjugacy class of g. With our convention, the conjugacy classes of A_4 are

$$\begin{aligned} C_0&=[1], & |C_0|&=1,\\ C_1&=[r_2], & |C_1|&=3,\\ C_2&=[r_3^2], & |C_2|&=4,\\ C_3&=[r_3], & |C_3|&=4, \end{aligned} \quad (77)$$

where r_2 and r_3 are defined in Eq. (23), and $|C|$ denotes the number of elements in a conjugacy class C. The class C_1 consists of the order-two elements, while C_2 and C_3 are the two conjugacy classes of order-three elements.

Let $\tilde{r}_2,\tilde{r}_3\in\tilde{A}_4$ be lifts of r_2, r_3, respectively,

$$p(\tilde{r}_2)=r_2, \qquad p(\tilde{r}_3)=r_3. \quad (78)$$

We choose them so that

$$\tilde{r}_2^2=-1, \qquad \tilde{r}_3^3=-1. \quad (79)$$

Thus $\tilde{r}_2$ has order four, and $\tilde{r}_3$ has order six. The conjugacy classes of $\tilde{A}_4$ are

$$\begin{aligned} D_0&=[1], & |D_0|&=1,\\ D_1&=[-1], & |D_1|&=1,\\ D_2&=[\tilde{r}_3], & |D_2|&=4,\\ D_3&=[\tilde{r}_3^{-1}], & |D_3|&=4,\\ D_4&=[\tilde{r}_3^2], & |D_4|&=4,\\ D_5&=[\tilde{r}_3^{-2}], & |D_5|&=4,\\ D_6&=[\tilde{r}_2], & |D_6|&=6. \end{aligned} \quad (80)$$

Under the covering map $p:\tilde{A}_4\to A_4$, these classes project as

$$\begin{aligned} D_0,D_1&\mapsto C0,\\ D_6&\mapsto C_1,\\ D_3,D_4&\mapsto C_2,\\ D_2,D_5&\mapsto C_3. \end{aligned} \quad (81)$$

For the order-two and order-three vortex families constructed above, the asymptotic $SO(3)$ holonomies are

$$U_N=r_2^N, \qquad U_M=r_3^M, \quad (82)$$

TABLE I. Topological classification of the two vortex families. The $SO(3)$ holonomy is classified by conjugacy classes $C_i \subset A_4$, while the full topological sector is classified by conjugacy classes $D_i \subset \tilde{A}_4 = p^{-1}(A_4)$.

Family	Vortex label	$SO(3)$ Holonomy class	Vortex Topological sector
Order-two	$N = 0$ mod 4	C_0	D_0
Order-two	$N = 1$ mod 4	C_1	D_6
Order-two	$N = 2$ mod 4	C_0	D_1
Order-two	$N = 3$ mod 4	C_1	D_6
Order-three	$M = 0$ mod 6	C_0	D_0
Order-three	$M = 1$ mod 6	C_3	D_2
Order-three	$M = 2$ mod 6	C_2	D_4
Order-three	$M = 3$ mod 6	C_0	D_1
Order-three	$M = 4$ mod 6	C_3	D_5
Order-three	$M = 5$ mod 6	C_2	D_3

respectively. Their topological classes are represented by $\tilde{r}_2^N$ and $\tilde{r}_3^M$. Since $\tilde{r}_2$ and $\tilde{r}_3$ have orders four and six, respectively, the classification depends on N mod 4 and M mod 6. The result is summarized in Table I.

In particular, the projected $SO(3)$ holonomy is trivial for $N = 2$ mod 4 and $M = 3$ mod 6, but the corresponding topological class is $D_1 = [-1]$. These configurations are therefore topologically nontrivial despite having trivial $SO(3)$ holonomy.

VI. RELATION TO NONINVERTIBLE ONE-FORM SYMMETRIES IN A_4 GAUGE THEORY

We now explain the relation between the vortices constructed above and the noninvertible one-form symmetry of the infrared A_4 gauge theory. At energies well below the mass scales m_+, m_-, and m_G, the massive Higgs and gauge fluctuations are integrated out, and the $SO(3) \to A_4$ Higgs phase is described by a discrete A_4 gauge theory. It is known that a finite-group gauge theory has a noninvertible one-form symmetry, whose topological surface operators are labeled by conjugacy classes of the gauge group [62,63]. These surface operators are often called Gukov-Witten operators.

Let us describe these operators in lattice language. In a lattice formulation of an A_4 gauge theory, a group element

$$U_{yx} \in A_4 \tag{83}$$

is assigned to each oriented link (y, x) from x to y with

$$U_{xy} = U_{yx}^{-1}. \tag{84}$$

For an oriented plaquette

$$\square = (x_0x_3)(x_3x_2)(x_2x_1)(x_1x_0), \tag{85}$$

one imposes the flatness condition

$$Hol_{x_0}(\square) \coloneqq U_{x_0x_3}U_{x_3x_2}U_{x_2x_1}U_{x_1x_0} = 1_{A_4}, \tag{86}$$

where 1_{A_4} is the identity element of A_4. The quantity $Hol_{x_0}(\square)$ is the finite-group analog of the continuum holonomy

$$\mathrm{P}\exp\left(-i\oint_{\partial\square} W_\mu dx^\mu\right). \tag{87}$$

Now let Σ be a codimension-two surface in spacetime, and let $\square$ be a plaquette linking Σ. For a fixed element $g \in A_4$, we define $T_g(\Sigma; x_0)$ as the insertion which changes the flatness condition on the linking plaquette to

$$\mathrm{Hol}_{x_0}(\square) = g. \tag{88}$$

Equivalently, $T_g(\Sigma; x_0)$ inserts a prescribed A_4 flux along Σ.

The operator $T_g(\Sigma; x_0)$ is not a physical surface operator by itself, because the holonomy is conjugated under a gauge transformation or a change of base point. Indeed, under a lattice gauge transformation

$$U_{xy} \longmapsto s_x U_{xy} s_y^{-1}, \qquad s_x \in A_4, \tag{89}$$

the plaquette holonomy transforms as

$$\mathrm{Hol}_{x_0}(\square) \mapsto s_{x_0}\,\mathrm{Hol}_{x_0}(\square)s_{x_0}^{-1}. \tag{90}$$

Similarly, if we change the base point, for example, from x_0 to x_1, then the same plaquette holonomy is written as

$$\begin{aligned}\mathrm{Hol}_{x_1}(\square) &= U_{x_1x_0}U_{x_0x_3}U_{x_3x_2}U_{x_2x_1} \\ &= U_{x_0x_1}^{-1}\mathrm{Hol}_{x_0}(\square)U_{x_0x_1}.\end{aligned} \tag{91}$$

Thus, changing the base point conjugates the plaquette holonomy.

As shown above, both gauge transformations and changes of base point conjugate the plaquette holonomy. Therefore, for a conjugacy class $C = [g] \subset A_4$, we can define a gauge-invariant and base-point-independent operator by summing over C:

$$T_C(\Sigma) \coloneqq \sum_{h\in C} T_h(\Sigma; x_0). \tag{92}$$

Indeed, conjugation merely permutes the elements of C, and hence only relabels the terms on the right-hand side, leaving the sum unchanged. The operators $T_C(\Sigma)$ are the Gukov-Witten operators. They are topological in the sense that their correlation functions are invariant under continuous deformations of Σ that do not cross other operator insertions.

TABLE II. Indicators associated with the Gukov-Witten surface operators for Wilson loops in the irreducible representations of A_4. Each entry gives the phase factor multiplying the corresponding Wilson loop when it links the surface operator once.

	T_{C_0}	T_{C_1}	T_{C_2}	T_{C_3}
$W_{\mathbf{1}}$	1	3	4	4
$W_{\mathbf{1}'}$	1	3	$4\omega^2$	4ω
$W_{\mathbf{1}''}$	1	3	4ω	$4\omega^2$
$W_{\mathbf{3}}$	1	−1	0	0

We next describe the action of these operators on Wilson loops. Let

$$\ell = (x_0x_n)(x_nx_{n-1})\cdots(x_2x_1)(x_1x_0) \tag{93}$$

be an oriented closed loop on the lattice based at x_0. The holonomy along ℓ is defined by

$$\mathrm{Hol}_{x_0}(\ell) \coloneqq U_{x_0x_n}U_{x_nx_{n-1}}\cdots U_{x_2x_1}U_{x_1x_0}. \tag{94}$$

The holonomy itself is neither gauge invariant nor base-point independent, since both gauge transformations and changes of base point act on it by conjugation. Taking the trace in a representation removes this conjugation dependence. Thus, for an irreducible representation $\mathcal{R}$ of A_4, we can define a gauge-invariant and base-point-independent operator by

$$W_{\mathcal{R}}(\ell) \coloneqq \mathrm{Tr}_{\mathcal{R}}\mathrm{Hol}_{x_0}(\ell). \tag{95}$$

This is the Wilson loop associated with $\mathcal{R}$, and it represents the worldline of a test particle transforming in the representation $\mathcal{R}$ of A_4.

When ℓ links Σ once, the Gukov-Witten operator acts on the Wilson loop as

$$T_C(\Sigma)\cdot W_{\mathcal{R}}(\ell) = \frac{|C|\chi_{\mathcal{R}}(C)}{\dim\mathcal{R}}W_{\mathcal{R}}(\ell), \tag{96}$$

where $\chi_{\mathcal{R}}(C)$ denotes the common value of the character in the conjugacy class C. Thus the Gukov-Witten surface operators act topologically on one-dimensional Wilson loops, with eigenvalues determined by the characters of A_4. These eigenvalues are the corresponding A_4 indicators. The collection of these surface operators generates the noninvertible one-form symmetry. Note that this one-form symmetry can be explicitly broken by adding dynamical matter fields that screen the Wilson loops [63].

Using the notation for the conjugacy classes introduced in Sec. V, the indicators in (96) are summarized in Table II. Here $\mathbf{1}$, $\mathbf{1}'$, $\mathbf{1}''$, and $\mathbf{3}$ label the irreducible representations of A_4. We use the convention

$$\mathbf{1}'(r_3) = \omega, \qquad \mathbf{1}''(r_3) = \omega^2, \qquad \omega = e^{2\pi i/3}. \tag{97}$$

The fusion rules of the Gukov-Witten operators are given by the conjugacy class algebra of A_4 and are summarized in Table III. Since fusing two such operators does not generally produce a single operator but rather a sum of operators, the corresponding one-form symmetry is noninvertible.

We now compare these infrared surface operators with the smooth vortices in the $SO(3)\to A_4$ Higgs theory. As explained in Sec. V, the smooth finite-tension vortices are classified by conjugacy classes of $\tilde{A}_4 = \pi_1(SO(3)/A_4)$. This classification contains UV information about how the fields wind in the continuous vacuum manifold $SO(3)/A_4$. In the infrared A_4 gauge theory, however, this detailed winding information is not retained in the effective description: only the A_4 holonomy around a linking circle remains, while the information distinguishing different lifts to $\tilde{A}_4$ is lost.

This observation naturally leads to a map from the conjugacy classes of $\tilde{A}_4$ to those of A_4. Using the notation of Sec. V, the covering map $p\colon SU(2)\to SO(3)$, restricted to $\tilde{A}_4\subset SU(2)$, induces a map on conjugacy classes,

$$[\tilde{g}]\longmapsto[p(\tilde{g})]. \tag{98}$$

A smooth vortex in the sector $[\tilde{g}]$ is therefore described in the infrared by the Gukov-Witten operator $T_{[p(\tilde{g})]}$. In other words, different $\tilde{A}_4$ sectors may become indistinguishable after flowing to the infrared A_4 gauge theory, if they have the same projected A_4 holonomy. For example, the two sectors D_3 and D_4 both project to C_2. Hence, vortices in either sector are described in the infrared by the same Gukov-Witten operator T_{C_2}. These two sectors are distinguished by the smooth-core structure of the $SO(3)\to A_4$ Higgs configuration, but this distinction is not visible in the infrared A_4 gauge theory.

Thus, the magnetic flux carried by each smooth finite-tension vortex constructed in this paper flows in the infrared to a Gukov-Witten surface operator in the A_4 gauge theory. In this sense, the $SO(3)$ gauge-Higgs model provides a smooth finite-tension UV realization of these infrared surface operators within a renormalizable field theory.

VII. DISCUSSION

In this article, the order-two and order-three vortex families have been analyzed within minimal cylindrically symmetric *Ansätze*. A notable feature of these solutions is the appearance of BPS-like points: $\kappa = 1$ for the order-two family and $(\eta,\kappa) = (1,1)$ for the order-three family. At these points, the reduced equations and energy functionals take the same form as those of the Abelian-Higgs model at its Bogomol'nyi point. It follows that static multivortex configurations can exist with no binding energy, as in the

TABLE III. Fusion rules of Gukov-Witten surface operators in A_4 gauge theory. Here C_0, C_1, C_2, C_3 are the conjugacy classes of A_4 defined in Sec. V. A similar fusion rule can be found in Refs. [37,43] for $G = U(1) \times SO(3)$ with spin-2 complex Higgs fields.

$\times$	T_{C_0}	T_{C_1}	T_{C_2}	T_{C_3}
T_{C_0}	T_{C_0}	T_{C_1}	T_{C_2}	T_{C_3}
T_{C_1}	T_{C_1}	$3T_{C_0} + 2T_{C_1}$	$3T_{C_2}$	$3T_{C_3}$
T_{C_2}	T_{C_2}	$3T_{C_2}$	$4T_{C_3}$	$4T_{C_0} + 4T_{C_1}$
T_{C_3}	T_{C_3}	$3T_{C_3}$	$4T_{C_0} + 4T_{C_1}$	$4T_{C_2}$

ordinary BPS Abelian-Higgs theory. In this sense, the vortices constructed above are BPS-like. This BPS-like property, however, is a statement within the reduced *Ansatz*: although the energy saturates the corresponding Bogomol'nyi bound in this sector, fluctuations outside the *Ansatz* may still lower the energy. This question is directly related to the stability of the BPS-like vortices constructed here, and we leave it for future work.

We next clarify how the global structure of the gauge group affects the interpretation of the vortices. At the local level, one may replace $SO(3)$ by $SU(2)$, since the two theories have the same Lie algebra. The local Lagrangian and the radial vortex equations are therefore unchanged. The global interpretation, however, is different. In the $SU(2)$ theory, the Higgs phase is

$$SU(2) \longrightarrow \tilde{A}_4, \tag{99}$$

rather than $SO(3) \to A_4$. Consequently, the infrared discrete gauge theory is a $\tilde{A}_4$ gauge theory.

It is also natural to ask how this construction extends to other finite subgroups of $SO(3)$. The same strategy should apply to other Higgs phases

$$SO(3) \to \Gamma, \tag{100}$$

where Γ is a finite subgroup of $SO(3)$. In such phases, one expects smooth vortices whose asymptotic holonomies lie in Γ, in direct analogy with the A_4 vortices constructed in this article. For example, even within the spin-3 representation, a different choice of renormalizable $SO(3)$-invariant potential can lead to the dihedral group $D_3 \simeq S_3$ as the residual symmetry. Other polyhedral groups can be realized by using higher-spin Higgs fields. In particular, spin-4 and spin-6 Higgs fields, together with suitable renormalizable $SO(3)$-invariant potentials, naturally realize S_4 and A_5 as residual symmetries, respectively [58–60]. For a general finite subgroup $\Gamma \subset SO(3)$, the topological classification of smooth vortices takes the universal form

$$\pi_1(SO(3)/\Gamma) = p^{-1}(\Gamma) \subset SU(2), \tag{101}$$

where $p: SU(2) \to SO(3)$ is the double covering map. Thus, the UV topological sectors are classified by the binary lift of the residual finite group. It would be interesting to understand whether the BPS-like behavior found in this article persists for other choices of Γ. The existence of such a point is not automatic. Unlike the topological classification above, it depends on the detailed structure of the Higgs representation and the choice of invariant potential.

There are several avenues for future work. First, an application to cosmic strings is one of the important future directions. When two cosmic strings characterized by commutative elements of the fundamental group collide, they pass through or reconnect with each other. Thus, cosmic strings can reduce their number, reaching the standard scaling law. On the other hand, when two cosmic strings corresponding to noncommutative elements of the fundamental group collide, a bridge is created between them [28,29,34,40]. As a consequence, the number of cosmic strings is not reduced during cosmic expansion, and a cosmic string network is inevitably formed [15], in which S_3 cosmic strings were explicitly discussed. Our construction provides a concrete framework for studying the dynamics, fusion, and interactions of non-Abelian cosmic strings in a fully renormalizable gauge theory.

A_4 vortices can be obtained in a $U(1) \times SO(3)$ gauge theory with spin-2 (complex) Higgs fields [33,34,37,40] instead of spin-3 Higgs fields studied in this article. In such a case, the fundamental group is some product of A_4 and $\mathbb{Z}$ [64]. Consequently, BPS A_4 vortices would satisfy the mass-charge relations, and would be $1/2$ BPS states when embedded into supersymmetric gauge theory. An analogous case is that a $U(1) \times SO(3)$ supersymmetric gauge theory with spin-1 (complex) Higgs fields admits $1/2$ BPS Alice strings [65,66],[3] as an extension of an $SO(3)$ gauge theory with spin-2 (real) Higgs fields [70].

When noninvertible defects create linkings, a noninvertible symmetry gives a selection rule for linkings, as explicitly shown for axion electrodynamics [71]. As compact noninvertible defects, non-Abelian vortex knots and links have thus far been constructed *ad hoc* [13,38–40]. In particular, in Ref. [40], all possible knots and links are classified for A_4 vortices. The noninvertible symmetry may provide a general framework for the construction of such compact noninvertible defects.

Finally, there are many important directions, such as quantum computation, finite temperature, finite density, and monopole attachment.

ACKNOWLEDGMENTS

This work is supported by JST Grant No. JPMJPF2221 (Y. A.), by JSPS KAKENHI Grants No. JP22K03601 (T. H.), No. JP22H01221 and No. JP23K22492 (M. N.),

[3] See Refs. [67–69] for global analogs for these strings.

No. JP25K17394 (R. Y.), and by the WPI program "Sustainability with Knotted Chiral Meta Matter (WPI-SKCM^2)" at Hiroshima University (M. N.).

DATA AVAILABILITY

There are no publicly available research data or software supporting this manuscript. Requests for further information or data should be sent to the authors.

APPENDIX A: LIE ALGEBRA GENERATORS IN THE SPIN-3 REPRESENTATION

In the orthonormal basis $e_1, \ldots, e_7$ of $\mathcal{H}_3$, the representation matrices X_a of the Lie algebra in the spin-3 representation are given by

$$X_1 = \begin{pmatrix} 0 & 0 & 0 & 0 & 0 & 0 & 0 \\ 0 & 0 & -3/2 & 0 & 0 & -\sqrt{15}/2 & 0 \\ 0 & 3/2 & 0 & 0 & -\sqrt{15}/2 & 0 & 0 \\ 0 & 0 & 0 & 0 & 0 & 0 & 2 \\ 0 & 0 & \sqrt{15}/2 & 0 & 0 & 1/2 & 0 \\ 0 & \sqrt{15}/2 & 0 & 0 & -1/2 & 0 & 0 \\ 0 & 0 & 0 & -2 & 0 & 0 & 0 \end{pmatrix}, \tag{A1}$$

$$X_2 = \begin{pmatrix} 0 & 0 & 3/2 & 0 & 0 & -\sqrt{15}/2 & 0 \\ 0 & 0 & 0 & 0 & 0 & 0 & 0 \\ -3/2 & 0 & 0 & -\sqrt{15}/2 & 0 & 0 & 0 \\ 0 & 0 & \sqrt{15}/2 & 0 & 0 & -1/2 & 0 \\ 0 & 0 & 0 & 0 & 0 & 0 & 2 \\ \sqrt{15}/2 & 0 & 0 & 1/2 & 0 & 0 & 0 \\ 0 & 0 & 0 & 0 & -2 & 0 & 0 \end{pmatrix}, \tag{A2}$$

$$X_3 = \begin{pmatrix} 0 & -3/2 & 0 & 0 & -\sqrt{15}/2 & 0 & 0 \\ 3/2 & 0 & 0 & -\sqrt{15}/2 & 0 & 0 & 0 \\ 0 & 0 & 0 & 0 & 0 & 0 & 0 \\ 0 & \sqrt{15}/2 & 0 & 0 & 1/2 & 0 & 0 \\ \sqrt{15}/2 & 0 & 0 & -1/2 & 0 & 0 & 0 \\ 0 & 0 & 0 & 0 & 0 & 0 & 2 \\ 0 & 0 & 0 & 0 & 0 & -2 & 0 \end{pmatrix}. \tag{A3}$$

APPENDIX B: EXPLICIT FORM OF THE QUARTIC INVARIANT

In this appendix we give the explicit component expression of the quartic $SO(3)$-invariant polynomial Q defined in Sec. II. Writing

$$\phi = \sum_{A=1}^{7} \phi_A e_A, \tag{B1}$$

one finds

$$Q(\phi) = \frac{1}{675}\Big(8(-2\phi_1^2+\phi_2^2-\sqrt{15}\phi_2\phi_5+\phi_3^2+\sqrt{15}\phi_3\phi_6)^2 + 8(\phi_1^2-\sqrt{15}\phi_1\phi_4+\phi_2^2+\sqrt{15}\phi_2\phi_5-2\phi_3^2)^2 + 8(\phi_1^2+\sqrt{15}\phi_1\phi_4-2\phi_2^2+\phi_3^2-\sqrt{15}\phi_3\phi_6)^2 + (3\phi_1\phi_2+\sqrt{15}\phi_1\phi_5-\sqrt{15}\phi_2\phi_4+4\sqrt{15}\phi_3\phi_7+15\phi_4\phi_5)^2 + (3\phi_1\phi_3-\sqrt{15}\phi_1\phi_6+4\sqrt{15}\phi_2\phi_7+\sqrt{15}\phi_3\phi_4+15\phi_4\phi_6)^2 + (4\sqrt{15}\phi_1\phi_7+3\phi_2\phi_3+\sqrt{15}\phi_2\phi_6-\sqrt{15}\phi_3\phi_5+15\phi_5\phi_6)^2\Big). \tag{B2}$$

Since the right-hand side is written as a sum of squares, this expression makes the non-negativity of Q manifest:

$$Q(\phi) \geq 0. \tag{B3}$$

It is also useful to relate this expression to the standard tensorial description of the spin-3 representation. An element of $\mathcal{H}_3$ can equivalently be represented by a totally symmetric traceless rank-three tensor D_{ijk}. Here "traceless" means that the contraction of any two indices with the Euclidean metric vanishes:

$$\delta^{ij}D_{ijk} = 0. \tag{B4}$$

Because D_{ijk} is totally symmetric, this condition is independent of which pair of indices is contracted. The corresponding harmonic polynomial is

$$\phi(\mathcal{X}) = D_{ijk}\mathcal{X}_i\mathcal{X}_j\mathcal{X}_k, \quad \mathcal{X} = (\mathcal{X}_1,\mathcal{X}_2,\mathcal{X}_3) = (\mathcal{X},\mathcal{Y},\mathcal{Z}), \tag{B5}$$

where repeated indices are summed over i, j, $k = 1, 2, 3$. The traceless condition is precisely the condition that this polynomial is harmonic, $\Delta\phi = 0$. Explicitly, in the basis used in this paper,

$$\begin{aligned}
D_{111} &= \sqrt{7}\phi_1,\\
D_{112} &= -\frac{\sqrt{7}}{2}\phi_2 - \frac{\sqrt{105}}{6}\phi_5,\\
D_{113} &= -\frac{\sqrt{7}}{2}\phi_3 + \frac{\sqrt{105}}{6}\phi_6,\\
D_{122} &= -\frac{\sqrt{7}}{2}\phi_1 + \frac{\sqrt{105}}{6}\phi_4,\\
D_{123} &= \frac{\sqrt{105}}{6}\phi_7,\\
D_{133} &= -\frac{\sqrt{7}}{2}\phi_1 - \frac{\sqrt{105}}{6}\phi_4,\\
D_{222} &= \sqrt{7}\phi_2,\\
D_{223} &= -\frac{\sqrt{7}}{2}\phi_3 - \frac{\sqrt{105}}{6}\phi_6,\\
D_{233} &= -\frac{\sqrt{7}}{2}\phi_2 + \frac{\sqrt{105}}{6}\phi_5,\\
D_{333} &= \sqrt{7}\phi_3,
\end{aligned} \tag{B6}$$

with all other components determined by total symmetry, $D_{ijk} = D_{(ijk)}$.

Under the above identification between ϕ and D_{ijk}, the invariants used in Sec. II are related to the tensor invariants by

$$I_2(\phi) = \frac{2}{35}J_2(D), \tag{B7}$$

$$Q(\phi) = \frac{8}{11025}(3J_4(D) - J_2(D)^2), \tag{B8}$$

where

$$J_2(D) \coloneqq D_{ijk}D_{ijk}, \tag{B9}$$

$$J_4(D) \coloneqq D_{ijk}D_{ij\ell}D_{pqk}D_{pq\ell}. \tag{B10}$$

APPENDIX C: UNIQUENESS OF THE b-PROFILE AT $\eta = 1$

In this appendix we prove that, at $\eta = 1$, the b-profile in the order-three vortex *Ansatz* is uniquely fixed by the boundary conditions required for finite tension and regularity.

At $\eta = 1$, the equation of motion for b decouples from the other profile functions and becomes

$$b'' = -\frac{b'}{R} + 2\kappa^2(b^2-1)b. \tag{C1}$$

The boundary conditions for b are

$$b'(0) = 0, b(\infty) = 1. \tag{C2}$$

The constant profile $b(R) \equiv 1$ is clearly a solution. We now show that it is the only finite-tension solution satisfying these boundary conditions.

Define

$$T(R) \coloneqq \frac{1}{2}(b')^2 - \frac{\kappa^2}{2}(b^2-1)^2. \tag{C3}$$

Using (C1), we find

$$T' = b'b'' - 2\kappa^2 b(b^2-1)b' = -\frac{(b')^2}{R} \leq 0. \tag{C4}$$

Thus $T(R)$ is nonincreasing. At the origin, the boundary condition gives

$$T(0) = -\frac{\kappa^2(b(0)^2-1)^2}{2} \leq 0. \tag{C5}$$

On the other hand, finite tension implies $b(R) \to 1$ and $b'(R) \to 0$ as $R \to \infty$, as follows from the b-dependent potential term and the positive $(b')^2$ term in (70). Hence $T(\infty) = 0$. Since T is nonincreasing, we have

$$0 = T(\infty) \leq T(R) \leq T(0) \leq 0. \tag{C6}$$

Therefore $T(R) \equiv 0$. In particular,

$$T'(R) = -\frac{(b')^2}{R} = 0 \tag{C7}$$

for all $R > 0$. Hence $b'(R) \equiv 0$, so b is constant. The boundary condition $b(\infty) = 1$ then gives $b(R) \equiv 1$.

This proves the uniqueness of the b-profile at $\eta = 1$.

APPENDIX D: NUMERICAL TEST AT THE BPS-LIKE POINT

The analytic result (68) provides a useful benchmark for testing the numerical calculation. We consider $N = 1$ and $\kappa = 1$, for which $E_2(1;1) = 1$. Denoting the numerically evaluated tension by $E_2^{\rm num}(1;1)$, we define the relative error as

$$\delta E = \frac{|E_2^{\rm num}(1;1) - E_2(1;1)|}{E_2(1;1)} = |E_2^{\rm num}(1;1) - 1|. \tag{D1}$$

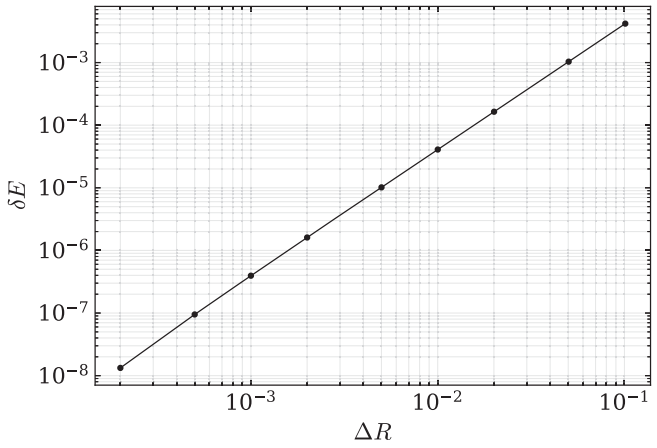


FIG. 5. Relative error δE of the numerical tension as a function of the radial grid spacing ΔR at $N = 1$ and $\kappa = 1$.

Figure 5 shows δE as a function of the radial grid spacing ΔR. The relative error decreases as ΔR is reduced.

[1] A. Vilenkin and E. P. S. Shellard, *Cosmic Strings and Other Topological Defects* (Cambridge University Press, Cambridge, England, 2000).

[2] N. S. Manton and P. Sutcliffe, *Topological Solitons*, Cambridge Monographs on Mathematical Physics (Cambridge University Press, Cambridge, England, 2004).

[3] E. J. Weinberg, *Classical solutions in Quantum Field Theory*: Solitons and Instantons in High Energy Physics, Cambridge Monographs on Mathematical Physics (Cambridge University Press, Cambridge, England, 2012).

[4] A. A. Abrikosov, On the Magnetic Properties of Superconductors of the Second Group, Sov. Phys. JETP **5**, 1174 (1957), https://jetp.ras.ru/cgi-bin/e/index/e/5/6/p1174?a=list.

[5] H. B. Nielsen and P. Olesen, Vortex line models for dual strings, Nucl. Phys. **B61**, 45 (1973).

[6] F. A. Bais, Flux metamorphosis, Nucl. Phys. **B170**, 32 (1980).

[7] M. G. Alford, K. Benson, S. R. Coleman, J. March-Russell, and F. Wilczek, The interactions and excitations of nonabelian vortices, Phys. Rev. Lett. **64**, 1632 (1990); **65**, 668 (E) (1990).

[8] F. Wilczek and Y.-S. Wu, Space-time approach to holonomy scattering, Phys. Rev. Lett. **65**, 13 (1990).

[9] M. G. Alford, K. Benson, S. R. Coleman, J. March-Russell, and F. Wilczek, Zero modes of nonabelian vortices, Nucl. Phys. **B349**, 414 (1991).

[10] M. G. Alford, K.-M. Lee, J. March-Russell, and J. Preskill, Quantum field theory of nonAbelian strings and vortices, Nucl. Phys. **B384**, 251 (1992).

[11] M. Bucher, K.-M. Lee, and J. Preskill, On detecting discrete Cheshire charge, Nucl. Phys. **B386**, 27 (1992).

[12] H.-K. Lo and J. Preskill, NonAbelian vortices and nonAbelian statistics, Phys. Rev. D **48**, 4821 (1993).

[13] L. Brekke, H. Dykstra, S. J. Hughes, and T. D. Imbo, Knots and links of nonabelian string, Phys. Lett. B **288**, 273 (1992).

[14] L. Brekke, S. J. Collins, and T. D. Imbo, NonAbelian vortices on surfaces and their statistics, Nucl. Phys. **B500**, 465 (1997).

[15] P. McGraw, Evolution of a nonAbelian cosmic string network, Phys. Rev. D **57**, 3317 (1998).

[16] A. Hanany and D. Tong, Vortices, instantons and branes, J. High Energy Phys. 07 (2003) 037.

[17] R. Auzzi, S. Bolognesi, J. Evslin, K. Konishi, and A. Yung, NonAbelian superconductors: Vortices and confinement in $N = 2$ SQCD, Nucl. Phys. **B673**, 187 (2003).

[18] M. Eto, Y. Isozumi, M. Nitta, K. Ohashi, and N. Sakai, Moduli space of non-Abelian vortices, Phys. Rev. Lett. **96**, 161601 (2006).

[19] M. Eto, K. Konishi, G. Marmorini, M. Nitta, K. Ohashi, W. Vinci, and N. Yokoi, Non-Abelian vortices of higher winding numbers, Phys. Rev. D **74**, 065021 (2006).

[20] M. Eto, Y. Isozumi, M. Nitta, K. Ohashi, and N. Sakai, Solitons in the Higgs phase: The Moduli matrix approach, J. Phys. A **39**, R315 (2006).

[21] M. Shifman and A. Yung, *Supersymmetric Solitons* (Cambridge University Press, Cambridge, England, 2009).

[22] A. P. Balachandran, S. Digal, and T. Matsuura, Semi-superfluid strings in high density QCD, Phys. Rev. D **73**, 074009 (2006).

[23] E. Nakano, M. Nitta, and T. Matsuura, Non-Abelian strings in high density QCD: Zero modes and interactions, Phys. Rev. D **78**, 045002 (2008).

[24] M. Eto and M. Nitta, Color magnetic flux tubes in dense QCD, Phys. Rev. D **80**, 125007 (2009).

[25] M. Eto, E. Nakano, and M. Nitta, Effective world-sheet theory of color magnetic flux tubes in dense QCD, Phys. Rev. D **80**, 125011 (2009).

[26] M. Eto, M. Nitta, and N. Yamamoto, Instabilities of non-Abelian vortices in dense QCD, Phys. Rev. Lett. **104**, 161601 (2010).

[27] M. Eto, Y. Hirono, M. Nitta, and S. Yasui, Vortices and other topological solitons in dense quark matter, Prog. Theor. Exp. Phys. **2014**, 012D01 (2014).

[28] N. D. Mermin, The topological theory of defects in ordered media, Rev. Mod. Phys. **51**, 591 (1979).

[29] V. Poenaru and G. Toulouse, The crossing of defects in ordered media and the topology of 3-manifolds, J. Phys. (Paris) **38**, 887 (1977).

[30] G. E. Volovik and V. P. Mineev, Investigation of singularities in superfluid He3 and in liquid crystals by the homotopic topology methods, Zh. Eksp. Teor. Fiz. **72**, 2256 (1977) [Sov. Phys. JETP **45**, 1186 (1977)], https://jetp.ras.ru/cgi-bin/e/index/e/45/6/p1186?a=list.

[31] A. P. Balachandran, F. Lizzi, and V. G. J. Rodgers, Topological symmetry breakdown in cholesterics, nematics, and ^{3}He, Phys. Rev. Lett. **52**, 1818 (1984).

[32] O. D. Lavrentovich and M. Kleman, Cholesteric liquid crystals: Defects and topology, in *Chirality in Liquid Crystals*, edited by H.-S. Kitzerow and C. Bahr (Springer, New York, 2001), pp. 115–158.

[33] G. W. Semenoff and F. Zhou, Discrete symmetries and 1/3-quantum vortices in condensates of $F = 2$ cold atoms, Phys. Rev. Lett. **98**, 100401 (2007).

[34] M. Kobayashi, Y. Kawaguchi, M. Nitta, and M. Ueda, Collision dynamics and rung formation of non-Abelian vortices, Phys. Rev. Lett. **103**, 115301 (2009).

[35] Y. Kawaguchi and M. Ueda, Spinor Bose-Einstein condensates, Phys. Rep. **520**, 253 (2012).

[36] M. O. Borgh and J. Ruostekoski, Core structure and non-Abelian reconnection of defects in a biaxial nematic spin-2 Bose-Einstein condensate, Phys. Rev. Lett. **117**, 275302 (2016).

[37] T. Mawson, T. Petersen, J. Slingerland, and T. Simula, Braiding and fusion of non-Abelian vortex anyons, Phys. Rev. Lett. **123**, 140404 (2019).

[38] T. Annala, R. Zamora-Zamora, and M. Möttönen, Topologically protected vortex knots and links, Communications Physics **5**, 309 (2022).

[39] H. Rajamäki, T. Annala, and M. Möttönen, Topologically protected vortex knots in an experimentally realizable system, Phys. Rev. Lett. **133**, 236604 (2024).

[40] M. Kobayashi, Y. Nozaki, Y. Koda, and M. Nitta, Quantum knots that never come untied, arXiv:2410.07470.

[41] K. Masuda and M. Nitta, Half-quantized non-Abelian vortices in neutron $^3P_2$ superfluids inside magnetars, Prog. Theor. Exp. Phys. **2020**, 013D01 (2020).

[42] Y. Masaki, T. Mizushima, and M. Nitta, Non-Abelian half-quantum vortices in ^{3}P$_2$ topological superfluids, Phys. Rev. B **105**, L220503 (2022).

[43] Y. Masaki, T. Mizushima, and M. Nitta, Non-Abelian anyons and non-Abelian vortices in topological superconductors, in *Encyclopedia of Condensed Matter Physics*, vol. 2 (Elsevier, New York, 2024), 2nd ed., pp. 755–794.

[44] M. Kobayashi and M. Nitta, Core structures of vortices in Ginzburg-Landau theory for neutron $^3P_2$ superfluids, Phys. Rev. C **105**, 035807 (2022).

[45] M. Kobayashi and M. Nitta, Proximity effects of vortices in neutron ^{3}P$_2$ superfluids in neutron stars: Vortex core transitions and covalent bonding of vortex molecules, Phys. Rev. C **107**, 045801 (2023).

[46] G. Marmorini, S. Yasui, and M. Nitta, Pulsar glitches from quantum vortex networks, Sci. Rep. **14**, 7857 (2024).

[47] T. Hattori, M. Nitta, and K. Sekizawa, Formation of bound composite vortices of a singly-quantized ^{1}S$_0$ vortex and half-quantized ^{3}P$_2$ vortices in the ^{1}S$_0$-^{3}P$_2$ coexisting phase in neutron stars, arXiv:2605.28718.

[48] P. A. Horvathy, The nonabelian Aharonov-Bohm effect, Phys. Rev. D **33**, 407 (1986).

[49] R. Sundrum and L. J. Tassie, Nonabelian Aharonov-Bohm effects, Feynman paths, and topology, J. Math. Phys. (N.Y.) **27**, 1566 (1986).

[50] M. G. Alford, J. March-Russell, and F. Wilczek, Discrete quantum hair on black holes and the nonabelian Aharonov-Bohm effect, Nucl. Phys. **B337**, 695 (1990).

[51] J. Preskill and L. M. Krauss, Local discrete symmetry and quantum mechanical hair, Nucl. Phys. **B341**, 50 (1990).

[52] F. A. Bais, P. van Driel, and M. de Wild Propitius, Quantum symmetries in discrete gauge theories, Phys. Lett. B **280**, 63 (1992).

[53] F. A. Bais, P. van Driel, and M. de Wild Propitius, Anyons in discrete gauge theories with Chern-Simons terms, Nucl. Phys. **B393**, 547 (1993).

[54] L. M. Krauss and F. Wilczek, Discrete gauge symmetry in continuum theories, Phys. Rev. Lett. **62**, 1221 (1989).

[55] G. Altarelli and F. Feruglio, Discrete flavor symmetries and models of neutrino mixing, Rev. Mod. Phys. **82**, 2701 (2010).

[56] F. Feruglio, *Are Neutrino Masses Modular Forms?* (World Scientific, Singapore, 2019), pp. 227–266.

[57] H. Ishimori, T. Kobayashi, H. Ohki, Y. Shimizu, H. Okada, and M. Tanimoto, Non-Abelian discrete symmetries in particle physics, Prog. Theor. Phys. Suppl. **183**, 1 (2010).

[58] B. A. Ovrut, Isotropy subgroups of $SO(3)$ and Higgs potentials, J. Math. Phys. (N.Y.) **19**, 418 (1978).

[59] G. Etesi, Spontaneous symmetry breaking in $SO(3)$ gauge theory to discrete subgroups, J. Math. Phys. (N.Y.) **37**, 1596 (1996).
[60] S. F. King and Y.-L. Zhou, Spontaneous breaking of $SO(3)$ to finite family symmetries with supersymmetry—an A_4 model, J. High Energy Phys. 11 (2018) 173.
[61] D. Gaiotto, A. Kapustin, N. Seiberg, and B. Willett, Generalized global symmetries, J. High Energy Phys. 02 (2015) 172.
[62] S. Gukov and E. Witten, Rigid surface operators, Adv. Theor. Math. Phys. **14**, 87 (2010).
[63] B. Heidenreich, J. McNamara, M. Montero, M. Reece, T. Rudelius, and I. Valenzuela, Non-invertible global symmetries and completeness of the spectrum, J. High Energy Phys. 09 (2021) 203.
[64] S. Kobayashi, M. Kobayashi, Y. Kawaguchi, M. Nitta, and M. Ueda, Abe homotopy classification of topological excitations under the topological influence of vortices, Nucl. Phys. **B856**, 577 (2012).
[65] C. Chatterjee and M. Nitta, BPS Alice strings, J. High Energy Phys. 09 (2017) 046.
[66] C. Chatterjee and M. Nitta, The effective action of a BPS Alice string, Eur. Phys. J. C **77**, 809 (2017).
[67] U. Leonhardt and G. E. Volovik, How to create Alice string (half quantum vortex) in a vector Bose-Einstein condensate, Pis'ma Zh. Eksp. Teor. Fiz. **72**, 66 (2000).
[68] R. Sato, F. Takahashi, and M. Yamada, Unified origin of axion and monopole dark matter, and solution to the domain-wall problem, Phys. Rev. D **98**, 043535 (2018).
[69] C. Chatterjee, T. Higaki, and M. Nitta, Note on a solution to domain wall problem with the Lazarides-Shafi mechanism in axion dark matter models, Phys. Rev. D **101**, 075026 (2020).
[70] A. S. Schwarz, Field theories with no local conservation of the electric charge, Nucl. Phys. **B208**, 141 (1982).
[71] Y. Hidaka, M. Nitta, and R. Yokokura, Selection rules of topological solitons from non-invertible symmetries in axion electrodynamics, J. High Energy Phys. 09 (2025) 082.